



## Enhancing the Sensitivity of Colorimetric Lateral Flow Assay (CLFA) through Signal Amplification Techniques

Journal:	<i>Journal of Materials Chemistry B</i>
Manuscript ID	TB-HIG-06-2018-001603.R1
Article Type:	Highlight
Date Submitted by the Author:	04-Jul-2018
Complete List of Authors:	Ye, Haihang; University of Central Florida, Chemistry Xia, Xiaohu; University of Central Florida, Chemistry

SCHOLARONE™  
Manuscripts

*Highlight to JMC B, 6/2018*

# **Enhancing the Sensitivity of Colorimetric Lateral Flow Assay (CLFA) through Signal Amplification Techniques**

Haihang Ye<sup>†</sup> and Xiaohu Xia<sup>†,\*</sup>

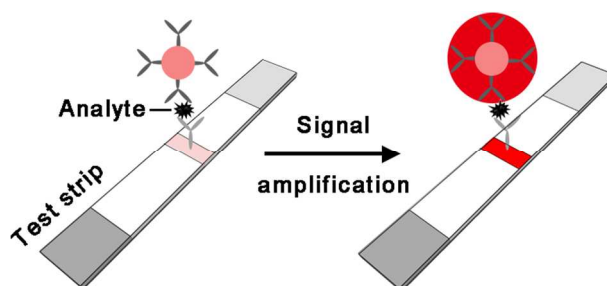
<sup>†</sup>*Department of Chemistry, University of Central Florida, Orlando, Florida 32816, United States*

\*Corresponding author. E-mail: [Xiaohu.Xia@ucf.edu](mailto:Xiaohu.Xia@ucf.edu)

## Abstract

Colorimetric lateral flow assay (CLFA) is one of a handful of diagnostic technologies that can be truly taken out of the laboratory for point-of-care testing without the needs of any equipment and skilled personnel. Despite the simplicity and practicality, it remains a grand challenge to substantially enhance the detection sensitivity of CLFA without adding complexity. Such a limitation in sensitivity inhibits many critical applications such as early detection of significant cancers and severe infectious diseases. With the rapid development of materials science and nanotechnology, signal amplification techniques that hold great potential to break through the existing detection limit barrier of CLFA have been developed in recent years. This article specifically highlights these emerging techniques for CLFA development. Rational, advantages, and limitations of each technique are discussed. Perspectives on future research directions in this niche and important field are provided.

## Table of Contents



This article highlights recent signal amplification techniques for enhancing the detection sensitivity of colorimetric lateral flow assay.

**Keywords:** Lateral flow assay · colorimetric detection · signal amplification · nanoparticle

## 1. Introduction

Lateral flow assay (LFA, also known as test strip) is one of the most widely used point-of-care diagnostic technologies owing to its simplicity, rapidness, and cost-effectiveness. The most commonly known LFA might be the "over-the-counter pregnancy test" that became commercially available in the 1980s.<sup>1,2</sup> Over the past several decades, a vast variety of LFAs have been developed for clinical, agricultural, bio-defensive, and environmental applications.<sup>3-9</sup>

A typical LFA works on a set of wettable materials that are assembled on a strip of plastic backing card (see Fig. 1a). All required chemicals and reagents are pre-stored in the test strip. Using antibodies as bioreceptors and "sandwich type" assay as a model system, Fig. 1b illustrates the general principle of a LFA. Other forms of LFA (*e.g.*, nucleic acids as bioreceptors and "competitive type" assay) and more technical details could be found in previously published comprehensive review articles.<sup>10-12</sup> Briefly, a small volume of sample applied to the sample pad flows across conjugate pad, nitrocellulose membrane, and absorbent pad in turn as driven by capillary forces. During this course, analytes are recognized by detection antibodies-conjugated nanoparticles (which are referred to as "labels"). The resulted analyte-label complexes are then captured by capture antibodies immobilized on the membrane to form test and control lines (see Fig. 1b). The concentration of analyte is proportional to the signal from labels accumulated in the test line region. Note the control line is designed to indicate the validity of test strip.

Since nanoparticle labels are responsible for signal generation, they largely determine the category and performance of a LFA. Up to date, various LFAs based on labels of different signal-transducer principles (*e.g.*, colorimetric,<sup>13,14</sup> fluorescent,<sup>15,16</sup> magnetic,<sup>17</sup> Raman scattering,<sup>18</sup> and chemiluminescent<sup>19</sup> labels) have been extensively developed. Among them, colorimetric LFA (CLFA) is particularly desired by the end users because it can be performed by a non-skilled person and quickly determined with the naked eye, without the requirement of any instrument. In contrast, most other LFAs are conducted with the assistance of complementary hardware and software, which more or less compromises the value of simplicity and low cost of LFAs. It should be noted that the majority of LFAs on the market are also CLFAs (most of them are based on gold nanoparticles as the labels). Significantly, CLFAs are urgently needed for diagnosing diseases and detecting pollution in resource-constrained areas or countries.

Nevertheless, the bottleneck of CLFA development is the relatively low detection sensitivity compared to other diagnostic technologies. This low sensitivity of CLFA inhibits many critical

applications. For example, it is expected that the mortality rates of severe infectious diseases such as Zika, Malaria, and Ebola could be greatly decreased if the diseases are detected in time by CLFAs.<sup>20-22</sup> Also, it is currently not feasible to apply CLFAs to detect significant cancers (*e.g.*, prostate and cervical cancers)<sup>23,24</sup> at early stages, because CLFA requires orders of magnitude more biomarkers than what exists in clinical samples. Taken together, it is of great importance and urgency to develop biosensing techniques that can substantially enhance the sensitivity of CLFAs.

It is known that the sensitivity of CLFA is essentially confined by the relatively weak color signal from the labels. Visible detection signal requires the accumulation of a large amount of colorimetric labels in the test line region of a CLFA.<sup>10,11</sup> With the rapid development of materials science and nanotechnology, the color signal from a label can be drastically amplified, making it feasible to break through the existing detection limit barrier of CLFA. This article highlights recent signal amplification techniques designed for enhancing the sensitivity of CLFA. It should be mentioned that, while not discussed in this article, developments of CLFA from those aspects other than signal amplification (*e.g.*, improvement of the qualities of bioreceptors, new materials for assembly of test strips, and control of flow rate) can also contribute to enhanced sensitivity of CLFA.<sup>25-28</sup>

For the sake of generality and consistency, in this article, we will focus on Au nanoparticle (AuNP) as a model colorimetric label for illustration. Note that AuNPs are used most frequently in CLFA because of their fascinating physicochemical properties and facile production in large scales. In particular, owing to a phenomenon called localized surface plasmon resonance (LSPR),<sup>29,30</sup> they offer intense color signal (red, in most cases) that is orders of magnitude stronger than the color from ordinary organic dyes.<sup>31</sup> The signal amplification techniques, as well as the perspectives provided in this article, may be extended to other colorimetric labels such as carbon nanoparticles,<sup>32,33</sup> dyed beads,<sup>34,35</sup> and other metal (oxide) nanoparticles<sup>36,37</sup>.

## **2. Signal Amplification Techniques**

### **2.1. Increasing the density of AuNPs around an analyte**

A straightforward means to enhance the sensitivity of AuNPs-based CLFA is to increase the density of AuNPs around an analyte in the test line region. In this way, the color signal of AuNPs can be enhanced since the collective molar extinction of AuNPs is enlarged.<sup>29</sup>

To achieve this idea, several strategies have been developed. One of them is to prepare AuNP aggregates as labels for CLFA. A notable example for AuNP aggregates preparation is to interconnect AuNPs by means of oligonucleotides as reported by Hu *et al.* (Fig. 2a).<sup>38</sup> Specifically, a pair of oligonucleotide sequences – an amplification probe and a complementary probe – were conjugated to two batches of AuNPs separately. AuNP aggregates were formed through the hybridization between the two probes. After functionalizing the AuNP aggregates with a detection probe as a bioreceptor, they can be used as labels for CLFA. Using a nucleic acid sequence of human immunodeficiency virus type 1 (HIV-1) as a model analyte, the AuNP aggregates-based CLFA could achieve a detection limit of 0.1 nM. In comparison, when individual AuNPs were employed as labels, the detection limit was increased to 0.25 nM, indicating a 2.5-fold enhancement in sensitivity by the AuNP aggregates. In addition to oligonucleotides, antibody pairs were also used to prepare AuNP aggregates and enhance the detection signal. For example, in a work by Rivas *et al.*,<sup>39</sup> AuNPs were conjugated to polyclonal secondary antibodies that recognizes anti-FITC antibodies. When the secondary antibodies-conjugated AuNPs were incubated with free anti-FITC antibodies in a solution, AuNP aggregates were formed because polyclonal nature of the secondary antibodies on AuNPs allowed for multiple binding to a primary antibody. Such AuNP aggregates as labels ensured enhanced color signal and resulted in a new CLFA with improved sensitivity.

In abovementioned strategy, AuNP aggregates were performed prior to the assay. In an alternative approach, AuNP aggregates were designed to form during the assay. For example, in a work reported by Choi *et al.*,<sup>40</sup> two batches of AuNPs with different sizes were collectively used as the labels – the small AuNPs were conjugated with anti-analyte antibodies and bovine serum albumin (BSA) as a blocking agent, while the big AuNPs were coated with anti-BSA antibodies (see Fig. 2b). These two AuNP labels were dispersed onto two separate conjugate pads in a single test strip. During an assay, the small labels will flow faster and be captured first on the test line. The big labels coming up late will then attach to the small ones through the binding between BSA and anti-BSA antibody, forming AuNP aggregates on the test line. Using troponin I as a model analyte, this design improved the sensitivity of CLFA by up to 100 times. The same approach has been applied to CLFA of small molecules in a competitive-type assay.<sup>41</sup> A similar concept was demonstrated by Ge *et al.*<sup>42</sup> In this case, instead of BSA, oligonucleotides (along with detection antibodies) were conjugated to AuNPs to form the first AuNP label. The second

AuNP label was prepared by functionalizing AuNPs with another kind of oligonucleotides that are complementary to those on the first label. During the assay, after the first AuNP label had been captured on the test and control lines, the second AuNP label in a solution was loaded to the strip to bind to the first one through hybridization of oligonucleotides. A 10-fold enhancement in sensitivity (relative to conventional AuNPs based CLFA) was demonstrated in detection of histone methylation.

Another strategy for increasing the density of AuNPs is to assemble as many AuNPs onto a carrier of larger size. For instance, in a recent work, Xu *et al.* demonstrated the use of silica nanorod (SiNR) as the carrier to load AuNPs and amplify the signal of CLFA (see Fig. 2c).<sup>43</sup> Specifically, a single SiNR of 200 nm in diameter and 3.4  $\mu\text{m}$  in length was capable of loading  $\sim 10^4$  AuNPs of 16.7 nm in diameter. Detection limit of the AuNPs-SiNR-based CLFA was lowered 50 times compared to conventional AuNPs-based CLFA when a sandwich-type assay of rabbit IgG was performed as a model test. Similar concept was demonstrated by using branched dendrimer as the carrier to load AuNPs.<sup>44</sup>

While this technique is straightforward, there are some limitations one may keep in mind. For example, in the strategy of forming AuNP aggregates, the uniformity in terms of both size and morphology of the AuNP aggregates should be important parameters to optimize. The uniformity of labels largely determines the reproducibility and sensitivity of final CLFA. In the strategy of using carriers to load AuNPs, one should balance the size of carriers and their loading capacity. In general, carriers of larger sizes are able to carry more AuNPs due to their greater surface area.<sup>45</sup> On the other hand, however, the large size of a carrier will slow down the migration of labels in strip membrane, thus increasing the testing time and causing high background signal. Meanwhile, it arises the steric effect for the binding of bioreceptors to analytes.

## 2.2. Enlarging particle size through silver or gold enhancement

Silver enhancement (a classic electroless plating process) is a traditional technique that has been extensively used for signal enhancement in biochemistry, especially in immunogold assays.<sup>46-49</sup> In this technique (see Fig. 3a), colloidal AuNPs act as catalysts to reduce  $\text{Ag}^+$  ions to metallic Ag at room temperature in the presence of a reducing agent (typically hydroquinone buffered to an acidic pH). The reduced Ag atoms are deposited on the surface of the AuNPs, during which particle size of AuNPs is enlarged by up to 5 orders of magnitude.<sup>46</sup>

Since the extinction coefficient of Au or Ag nanoparticles (which is correlated to the

visibility of color signal) is drastically enlarged as the increase of particle size<sup>31,50</sup>, silver enhancement technique is expected to be powerful in enhancing the color signal of AuNP labels and thus lowering the detection limit of AuNPs-based CLFAs. The pioneer work by Yang *et al.* first demonstrated the feasibility of coupling silver enhancement technique with AuNPs-based CLFA to enhance its sensitivity.<sup>51</sup> Specifically, the assay was designed on the basis of a sandwich immunoassay, in which abrin-a was chosen as a model analyte. After the performance of CLFA and the accumulation of AuNPs in the test line region of strip membrane, two additional pads that were pre-coated with AgNO<sub>3</sub> as a precursor to silver and citrate buffered hydroquinone as a reducing agent were placed above the membrane. Both pads were then infiltrated by water, activating the silver enhancement reaction on AuNPs. After silver enhancement (approximately in 10 minutes, at room temperature), red lines in test strips arose from AuNPs turned into black due to the deposition of silver on AuNPs. Visual detection limit of this technique coupled CLFA was much lower than that of conventional AuNPs-based CLFA (Fig. 3b). The sensitivity improvement of CLFA through silver enhancement technique has been attested by other research groups in detecting different analytes.<sup>52,53</sup> In a comprehensive study of various colorimetric labels by Linares *et al.*, silver enhancement technique was demonstrated to be able to enhance the sensitivity of CLFA by a factor of 10.<sup>32</sup>

The improvement of CLFA sensitivity achieved by silver enhancement technique is mainly attributed to the enlargement of nanoparticles that augments their visibility in the test line of a strip. Such a rationale could also be realized by a similar technique – "gold enhancement". In gold enhancement, AuNPs catalyze the localized reduction of a salt precursor to Au (*e.g.*, HAuCl<sub>4</sub>) by a reducing agent (*e.g.*, NH<sub>2</sub>OH·HCl<sup>54</sup>), during which the size of AuNPs is substantially increased. When coupled with gold enhancement technique, the sensitivity of AuNPs-based CLFA could be enhanced by several times (see an example in Fig. 3c).<sup>55</sup>

In both techniques, reduction and deposition of Ag or Au are localized on the surface of AuNPs through self-catalysis. In reality, however, the reduction reaction may also be catalyzed by certain substances other than AuNPs in the detection system because the reaction can be easily activated thermodynamically. As a result, new Ag or Au particles outside the initial AuNPs may form *via* homogeneous nucleation,<sup>56</sup> leading to the increase of background signal in CLFA tests and thus the decrease of sensitivity. In this regard, to achieve a desirable signal-to-noise ratio, one may need to consider eliminating the influence of matrices from samples and test strip



materials on the catalytic reactions during silver or gold enhancement.

It should be noted that the involvement of  $\text{Ag}^+$  or  $\text{Au}^{3+}$  ions in this signal enhancement strategy is a potential issue to consider. Both ions were found to adversely affect the environment and have serious biological effects on human health. For instance, exposure to  $\text{Ag}^+$  may lead to argyria and severe symptoms such as stomach distress and organ edema.<sup>57,58</sup>  $\text{Au}^{3+}$  was recognized to cause damages to liver, kidney, and peripheral nervous systems. Such a potential issue caused by these toxic ions needs to be somehow addressed, especially CLFAs are generally performed in non-laboratory scenarios.<sup>59,60</sup>

### 2.3. Modifying AuNP surface with enzymes

Enzymes are macromolecular biological catalysts that catalyze the conversion of substrates to products.<sup>61</sup> As a group of unique enzymes, peroxidases can effectively generate colored products by catalyzing chromogenic substrates. A single horseradish peroxidase (HRP, a commonly used peroxidase extracted from the roots of horseradish) is capable of yielding up to  $10^3$  colored products in one second.<sup>62</sup> Therefore, HRP has been widely used in colorimetric diagnostics and imaging technologies (*e.g.*, western blot and enzyme-linked immunosorbent assay), wherein HRPs are conjugated to bioreceptors and specifically generate color signal.<sup>63-65</sup>

Taking advantage of its high catalytic activity, HRP has been applied to CLFA technology to enhance the detection sensitivity. In general, AuNPs are coated with both HRP molecules and bioreceptors and then serve as labels for CLFA (see Fig. 4a). After a complete assay, the test strip is treated with a catalytic reaction solution containing HRP substrates. Signal amplification and thus low detection limit are achieved through HRP-catalyzed reactions, in which colored products with intensities higher than the color from AuNPs are generated in the test and control lines of a strip. Note, the colored products are insoluble chromogens that cannot be moved by the liquid flow during an assay.

In a sandwich-type CLFA of DNA analytes, Mao *et al.* conjugated AuNPs with both HRP molecules and DNA probes.<sup>66</sup> After the complete assay, a catalytic solution containing 3-amino-9-ethyl-carbazole (AEC) and  $\text{H}_2\text{O}_2$  was applied to the sample pad of test strip. The HRP-catalyzed reaction was allowed to proceed for 5 minutes, during which red colored products (*i.e.*, oxidized AEC) were formed on the test and control lines (Fig. 4b). Using this signal amplification strategy, detection sensitivity of CLFA was enhanced by 10 times. In a follow-on study by He *et al.*,<sup>67</sup> the performance of the HRP-assisted CLFA was further enhanced by

optimizing the recipe of HRP-AuNP-DNA probe conjugate preparation. It was found that sodium dodecyl sulfate and the immobilization order of HRP and DNA probes on AuNP surfaces played key roles in determining the sensitivity of CLFA.

In addition to nucleic acid analytes, the HRP-assisted signal enhancement strategy was also demonstrated in detecting protein analytes by Parolo *et al.*<sup>68</sup> Specifically, AuNPs were coated with HRP and antibodies. Human IgG as a model analyte was detected in a sandwich-type CLFA. Three different types of HRP substrates – 3,3',5,5'-tetramethylbenzidine (TMB), 3,3'-diaminobenzidine tetrahydrochloride (DAB), and AEC were tested and compared. It was found that the use of TMB and AEC as substrates of HRP allowed an improvement of CLFA sensitivity of about one order of magnitude compared to AuNPs-based CLFA without signal enhancement (Fig. 4c). In contrast, DAB was not able to produce appreciable increment in the sensitivity of CLFA. It is worth mentioning that TMB, among these three substrates, gave the best limit of quantification because TMB granted the highest contrast between the lines and the background than the others. In addition, the catalytic solution prepared with TMB is cheaper and more stable than those with AEC and DAB. Therefore, TMB was suggested to be the most suitable substrate for HRP-assisted CLFA.

In this technique, the improvement of CLFA sensitivity is considerable. The signal enhancement procedure is simple (*e.g.*, room temperature, aqueous solution, and 5-minute reaction time). Nevertheless, there are some drawbacks to take into consideration. For instance, the relatively poor thermal and chemical stabilities of enzymes is a potential issue,<sup>69,70</sup> which may shorten the shelf life of CLFA and affect the detection accuracy. Enzyme molecules will compete with bioreceptors for the surface area of a AuNP. The reduced loading amount of bioreceptors on AuNPs and the steric effect caused by the neighboring enzymes are likely to affect the efficiency of label in recognizing and binding to analytes. On the other hand, the loading amount of enzymes and thus the magnitude of signal amplification are confined by the limited surface area of a AuNP.<sup>45</sup>

#### **2.4. Coating AuNPs with a catalytic metal**

Within the past decade, nanoparticles made of platinum-group metals have been demonstrated to possess intrinsic peroxidase-like activities.<sup>71-75</sup> These nanoparticles as peroxidase mimics (or artificial peroxidases) provide two major advantages compared to their natural counterparts. First, their catalytic efficiency in terms of catalytic constant  $K_{cat}$ , which

measures the maximum number of chemical conversions of substrate molecules per second per enzyme or mimic, are much higher than natural peroxidases. For example,  $K_{\text{cat}}$  of  $\sim 20$  nm Pd-Ir nanoparticles is as high as  $10^6 \text{ s}^{-1}$ , while  $K_{\text{cat}}$  of HRP is only at the regime of  $10^3 \text{ s}^{-1}$ .<sup>62,72</sup> Second, they exhibit excellent stabilities owing to the inertness of noble metals. In contrast, natural peroxidases are relatively unstable since they are essentially made of proteins and therefore are subject to denaturation and protease digestion.<sup>76</sup> These two distinctive features make peroxidase mimics attractive to be integrated to CLFA, amplifying the detection signal and thus enhancing the sensitivity of CLFA.

In a recent work, our research group designed a novel label for CLFA by taking advantage of the superior peroxidase-like activity of Pt nanocrystals.<sup>77</sup> As shown by the schematics in Fig. 5a, conventional AuNPs of  $\sim 40$  nm in diameter as the seeds were coated with conformal, ultrathin shells of Pt to form unique Au@Pt<sub>*n*L</sub> core@shell NPs (*n*L: 1-10 atomic layers). The successful coating of Pt shells with controlled thicknesses at the atomic level relies on careful manipulations of the reaction kinetics during the synthesis. Au@Pt<sub>4L</sub> NPs as an example are shown in Fig. 5b, which will be used as a model sample in following discussions. We demonstrated that so long as the Pt shell was ultrathin (within several atomic layers), the plasmonic activity of the AuNP seeds underneath Pt would be well retained, making the resultant Au@Pt NPs as red as the initial AuNPs. On the other hand, Pt shells over AuNPs endowed the Au@Pt NPs with high peroxidase-like activities, allowing them to generate highly intense blue colored molecules (*i.e.*, oxidized TMB) within several minutes by catalyzing the reaction between TMB and H<sub>2</sub>O<sub>2</sub>. It should be emphasized that the intensity of blue color from catalysis was 3 orders of magnitude stronger (catalytic reaction time = 5 minutes) than that of the intrinsic red color from plasmonics, providing enhanced detection signal. Significantly, the surface properties (*e.g.*, chemical ligands and charge on the surface) of the Au@Pt NPs were similar to initial AuNPs, making it convenient to label antibodies on their surface using those well-established procedures for conventional AuNPs.

The dual functionalities, plasmonics and catalysis, along with the appropriate surface properties of the Au@Pt NPs make them extremely suitable for CLFA. They can offer two detection alternatives (see Fig. 5c): one produced just by the red color of AuNP cores (low-sensitivity mode) and the other more sensitive blue color generated from the Pt shells through catalysis (high-sensitivity mode), providing an "on-demand" tuning of the detection

performance. Note, the high-sensitivity mode is less straightforward than the low-sensitivity mode because it requires an additional signal enhancement procedure (*i.e.*, 5-minute treatment with TMB/H<sub>2</sub>O<sub>2</sub> catalytic solution at room temperature). Using human prostate-specific antigen (PSA) as a model analyte, the performance of Au@Pt NPs-based CLFA was evaluated. Fig. 5d compares the detection results of PSA standards in buffer solution using conventional AuNPs-based CLFA and Au@Pt NPs-based CLFA under low- and high-intensity modes. It can be seen that the naked eye detection limit was ~2 ng/mL for both AuNPs- and Au@Pt NPs-based CLFA (low-sensitivity mode). In contrast, a much lower detection limit of ~20 pg/mL was achieved by Au@Pt NPs-based CLFA under high-intensity mode, enhancing the sensitivity of CLFA by approximately 100 times. It is worth noting that the cost of Pt in this case should not be an issue to concern because the Pt shell on a AuNP is ultrathin (sub-10 atomic layers) and the materials usage of Au@Pt NPs in a CLFA test is rather tiny (at the level of microgram per test).<sup>77</sup>

Most recently, similar concept of signal amplification has been reported by Loynachan *et al.*<sup>78</sup> In this work, ~15 nm AuNPs as the seeds were coated with thick shells of Pt with rough surfaces to form ~120 nm Au@Pt NPs. The Au@Pt NPs were then functionalized with antibodies and used as labels for CLFA. Nanobody modified biotin-polystreptavidin system was employed to capture the target analyte. After completion of an assay, the strip was immersed in a solution containing peroxidase substrates (in this case, 4-chloro-1-naphthol/3,3'-diaminobenzidine tetrahydrochloride, CN/DAB, and H<sub>2</sub>O<sub>2</sub>). Pt shells on the surface possessing peroxidase-like activities were able to catalyzing the oxidation of CN/DAB by H<sub>2</sub>O<sub>2</sub>, yielding an insoluble black product which was clearly visible by the naked eye. An important biomarker – p24 as the viral capsid protein of human immunodeficiency virus (HIV) was detected. The sensitivity of such Au@Pt NPs-based CLFA was enhanced by 2 orders of magnitude after signal amplification through catalysis, enabling the detection of p24 down to a level of 0.8 pg/mL.

This signal amplification technique established by decorating AuNPs with Pt shells as peroxidase-mimicking materials is highly efficient. The storage and utilization of resultant Au@Pt core@shell NPs are similar to conventional AuNPs, making it straightforward to apply them to CLFA. In contrast to the approach achieved by coating AuNPs with enzymes (see section 2.3), this strategy is more robust because Pt shells are more catalytically active than enzymes in this particular case. In addition, Pt as a type of noble metal is more stable than enzymes. The extraordinary stability of Pt enables the label survive harsh environment, making the CLFA

suitable for on-site detection. The superior stabilities of Pt shells have been demonstrated in the work by Loynachan *et al.*<sup>78</sup> Notably, this signal amplification technique is not limited to Au@Pt NPs. Other nanoparticles with peroxidase-like activities are also applicable. For example, in the work by Jiang *et al.*, nanoparticles of Pt-Pd alloy have been employed as labels to enhance the sensitivity of CLFA.<sup>79</sup> It is worth noting that, in this technique, the nanoparticles used as labels may not be as compatible as AuNPs in CLFA platform. One needs to carefully control the surface properties of nanoparticles to ensure an efficient bioreceptor conjugation, low non-specific binding, and smooth migration across the membrane.

### 3. Summary and Outlook

In this article, we have highlighted recent signal amplification techniques that were designed to enhance the detection sensitivity of colorimetric lateral flow assay (CLFA). Au nanoparticles (AuNPs) as a model type of colorimetric label for CLFA were used for illustration. Specifically, four signal amplification techniques were elaborated: increasing the density of AuNPs around an analyte through particle aggregation, dual AuNP labels, and the use of AuNP carriers; enlarging the size of AuNPs by coupling with silver or gold enhancement; modifying AuNP surfaces with enzymes that can generate colored molecules by catalyzing chromogenic substrates; and coating AuNPs with a catalytic metal that serves as enzyme mimic. In the first two techniques, color signal from AuNPs themselves is enhanced (*via* particle enrichment and size enlargement). The latter two techniques rely on the generation of secondary color signal that is more intense than the primary color signal from AuNPs. Pros and cons of each technique have been discussed.

It should be mentioned that, while not focused in this article, those signal amplification techniques designed for labels other than AuNPs are also effective in improving the sensitivity of CLFA. For example, exonuclease III (Exo III) – an enzyme that can catalyze the stepwise removal of mononucleotides from 3'-hydroxyl terminus of double-stranded DNA – was used to establish a powerful signal amplification technique for CLFA.<sup>80</sup> With the assistance of Exo III, DNA probe along with analyte could be regenerate, resulting in the recycling of probe-analyte recognition event and the formation of amplified signal. In another example, cross-linking of polymers could be employed as a new mechanism for signal amplification. In a work by Liu *et al.*,<sup>81</sup> carboxyl groups-modified Fe<sub>3</sub>O<sub>4</sub> nanoparticles that present a dark brown color were prepared. Then, poly-L-lysine (PLL) was added to the Fe<sub>3</sub>O<sub>4</sub> nanoparticle suspension to induce

aggregation of  $\text{Fe}_3\text{O}_4$  nanoparticles through the cross-linking between carboxyl groups on particles and amine groups of PLL. The resultant aggregates of  $\text{Fe}_3\text{O}_4$  nanoparticles displayed enhanced color signal and resulted in a CLFA with improved sensitivity. Notably, in this method, the size of particle aggregates could be controlled by altering the ratio of nanoparticle to polymer.

While new techniques for enhancing the sensitivity of CLFA are being developed, one may take following aspects into consideration. Firstly, sensitivity and simplicity need to be balanced. In particular, since those diagnostic technologies with higher sensitivities than CLFA are available in resource-rich settings, simplicity as a unique feature of CLFA should not be compromised too much. Involvements of multiple steps, complicated procedures, and major instrument in a new technique are discouraged. Secondly, all the components of a test strip, including materials and reagents (see Fig. 1), as a whole have impacts on the sensitivity of a CLFA. In this regard, to achieve an optimized performance, innovation of one component may need to be associated with the adjustments of the others. For example, substitution of individual AuNPs as labels with AuNP aggregates could enhance the color signal of AuNPs. On the other hand, however, the large size of AuNP aggregates will slow down the migration of labels across the membrane, causing high background and thus a low signal-to-noise ratio.<sup>11</sup> This issue may be addressed by choosing a different type of membrane with larger pores. Thirdly, the influences of matrices from real samples on the performance of a new technique for CLFA need to be considered and evaluated. The matrices in a real sample are oftentimes rather complex and may cause unexpected side effects (*e.g.*, non-specific binding and noise signal). Such influences should be evaluated and eliminated through systematic optimizations, in which the test results may be benchmarked against those obtained from commercially available diagnostic kits. Fourthly, shelf life and stability of a new technique should be carefully assessed. In particular, since CLFAs are expected to be performed in non-laboratory scenarios, materials and methodologies that are invulnerable to the change of surrounding environments (*e.g.*, temperature, humidity, and pH value) are especially desired.

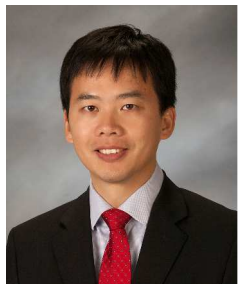
In view of future technological advancement, integrating the scientific discoveries and novel techniques from those emerging fields into CLFA might be a promising direction. For instance, with the rapid development of nanoscience and nanotechnology over the past few decades, it's now feasible to design and synthesize nanomaterials with precisely controlled sizes, shapes, and

compositions at the atomic level.<sup>82,83</sup> Those functional nanomaterials with outstanding properties may substantially enhance the performance of CLFAs. Moreover, nanomaterials with novel signal-transducer principles may create new opportunities for CLFA in the future.<sup>84-88</sup> High-tech microfluidic platforms that were developed in recent years hold great potential to be applied to CLFAs.<sup>89-91</sup> Through a set of fluidic unit operations, microfluidic platforms are able to finely tune the rate of liquid flows and the migration of nanoscale particles in a channel. Analytes of interest from a sample can be separated and concentrated by means of a microfluidic system. Moreover, microfluidics is extremely suitable for high-throughput screening applications. These capabilities of microfluidic technology make it promising candidate to be integrated to CLFA, lifting current limitations in CLFA. Recent advancement in optics and electronics also provide great opportunities to enhance the performance of CLFA.<sup>92-96</sup> For instance, the color signal of CLFA may be amplified and quantified by smart and portable electronic devices. We hope this article will serve as a useful source to inspire future research work in this niche field.

## Acknowledgements

This work was supported by the startup funds from University of Central Florida and a National Science Foundation (NSF) Career Award (CHE-1834874).

## Author Biography



Xiaohu Xia has been an Assistant Professor at University of Central Florida (UCF) since May 2018. He is a recipient of the U.S. NSF CAREER Award (class of 2017). Prior to his appointment at UCF, he worked at Michigan Technological University as an Assistant Professor from 2014-2018. He received his BS degree in biotechnology (2006) and PhD degree in biochemistry and molecular biology (2011) from Xiamen University, China.

He worked at Washington University in St. Louis as a Visiting Graduate student from 2009 to 2011 and at Georgia Tech as a Postdoctoral Fellow from 2012 to 2014. His research interests include the design and synthesis of novel nanostructures and exploration of their applications in biomedicine and catalysis.



Haihang Ye is currently a Ph.D. candidate in the department of chemistry at University of Central Florida (UCF). Before working at UCF, he was undertaking doctoral studies at Michigan Technological University from 2015-2018. He has been under the supervision of Prof. Xiaohu Xia since 2015. He received his B.S. in Material Chemistry (2012) and M.S. in Applied Chemistry (2015) from Beijing Jiaotong University, China. His research

focuses on the synthesis of functionalized nanomaterials for bio-sensing and catalytic applications.

## References

- 1 J. H. Leuvering, P. J. H. M. Thal, M. van der Waart and A. H. W. M. Schuurs, *J. immunoassay*, 1980, **1**, 77-91.
- 2 A. Vanamerongen, J. H. Wichers, L. B. J. M. Berendsen, A. J. M. Timmermans, G. D.



- Keizer, A. W. J. Vandoorn, A. Bantjes and W. M. J. Vangelder, *J. Biotechnol.*, 1993, **30**, 185-195.
- 3 Y. Xu, Y. Liu, Y. Wu, X. Xia, Y. Liao and Q. Li, *Anal. Chem.*, 2014, **86**, 5611-5614.
- 4 K. Glynnou, P. C. Ioannou, T. K. Christopoulos and V. Syriopoulou, *Anal. Chem.*, 2003, **75**, 4155-4160.
- 5 G. A. Kwong, G. Von Maltzahn, G. Murugappan, O. Abudayyeh, S. Mo, I. A. Papayannopoulos, D. Y. Sverdlov, S. B. Liu, A. D. Warren, Y. Popov and D. Schuppan, *Nat. biotechnol.*, 2013, **31**, 63.
- 6 R. H. Shyu, H. F. Shyu, H. W. Liu and S. S. Tang, *Toxicol.*, 2002, **40**, 255-258.
- 7 A. M. López Marzo, J. Pons, D. A. Blake and A. Merkoçi, *Anal. Chem.*, 2013, **85**, 3532-3538.
- 8 S. Shukla, H. Leem and M. Kim, *Anal. Bioanal. Chem.*, 2011, **401**, 2581-2590.
- 9 Y. A. Kim, E. H. Lee, K. O. Kim, Y. T. Lee, B. D. Hammock and H. S. Lee, *Anal. Chim. Acta*, 2011, **693**, 106-113.
- 10 G. A. Posthuma-Trumpie, J. Korf and A. van Amerongen, *Anal. Bioanal. Chem.*, 2009, **393**, 569-582.
- 11 D. Quesada-González and A. Merkoçi, *Biosens. Bioelectron.*, 2015, **73**, 47-63.
- 12 B. Ngom, Y. Guo, X. Wang and D. Bi, *Anal. Bioanal. Chem.*, 2010, **397**, 1113-1135.
- 13 A. M. Lopez-Marzo, J. Pons, D. A. Blake and A. Merkoçi, *Biosens. Bioelectron.*, 2013, **47**, 190-198.
- 14 W. Zhao, M. M. Ali, S. D. Aguirre, M. A. Brook and Y. Li, *Anal. Chem.*, 2008, **80**, 8431-8437.
- 15 Z. Li, Y. Wang, J. Wang, Z. Tang, J. Pounds and Y. Lin, *Anal. Chem.*, 2010, **82**, 7008-7014.
- 16 C. Liu, W. Ma, Z. Gao, J. Huang, Y. Hou, C. Xu, W. Yang and M. Gao, *J. Mater. Chem. C*, 2014, **2**, 9637-9642.
- 17 D. Wang, B. Tian, Z. Zhang, X. Wang, J. Fleming, L. Bi, R. Yang and X. Zhang, *Biosens. Bioelectron.*, 2015, **67**, 608-614.
- 18 X. Fu, Z. Cheng, J. Yu, P. Choo, L. Chen and J. Choo, *Biosens. Bioelectron.*, 2016, **78**, 530-537.
- 19 Y. Wang, C. Fill and S. R. Nugen, *Biosensors*, 2012, **2**, 32-42.
- 20 Gates, B., *N. Engl. J. Med.*, 2015, **372**, 1381-1384.

- 21 K. Pardee, A. A. Green, M. K. Takahashi, D. Braff, G. Lambert, J. W. Lee, T. Ferrante, D. Ma, N. Donghia, M. Fan and N. M. Daringer, *Cell*, 2016, **165**, 1255-1266.
- 22 R. G. Feachem, A. A. Phillips, J. Hwang, C. Cotter, B. Wielgosz, B. M. Greenwood, O. Sabot, M. H. Rodriguez, R. R. Abeyasinghe, T. A. Ghebreyesus and R. W. Snow, *Lancet*, 2010, **376**, 1566-1578.
- 23 R. De La Rica and M. M. Stevens, *Nat. Nanotechnol.*, 2012, **7**, 821-824.
- 24 M. H. Mayrand, E. Duarte-Franco, I. Rodrigues, S. D. Walter, J. Hanley, A. Ferenczy, S. Ratnam, F. Coutlée and E. L. Franco, *N. Engl. J. Med.*, 2007, **357**, 1579-1588.
- 25 R. Y. Chiu, E. Jue, A. T. Yip, A. R. Berg, S. J. Wang, A. R. Kivnick, P. T. Nguyen and D. T. Kamei, *Lab Chip*, 2014, **14**, 3021-3028.
- 26 J. Park, J. H. Shin and J. K. Park, *Anal. Chem.*, 2016, **88**, 3781-3788.
- 27 J. R. Choi, Z. Liu, J. Hu, R. Tang, Y. Gong, S. Feng, H. Ren, T. Wen, H. Yang, Z. Qu and B. Pingguan-Murphy, *Anal. Chem.*, 2016, **88**, 6254-6264.
- 28 L. Rivas, M. Medina-Sánchez, A. de la Escosura-Muñiz and A. Merkoçi, *Lab Chip*, 2014, **14**, 4406-4414.
- 29 X. Yang, M. Yang, B. Pang, M. Vara and Y. Xia, *Chem. Rev.*, 2015, **115**, 10410-10488.
- 30 S. Eustis and M. A. El-Sayed, *Chem. Soc. Rev.*, 2006, **35**, 209-217.
- 31 P. K. Jain, K. S. Lee, I. H. El-Sayed and M. A. El-Sayed, *J. Phys. Chem. B*, 2006, **110**, 7238-7248.
- 32 E. M. Linares, L. T. Kubota, J. Michaelis and S. Thalhammer, *J. Immunol. Methods*, 2012, **375**, 264-270.
- 33 M. Blažková, P. Rauch and L. Fukal, *Biosens. Bioelectron.*, 2010, **25**, 2122-2128.
- 34 N. Khreich, P. Lamourette, H. Boutal, K. Devilliers, C. Créminon and H. Volland, *Anal. biochem.*, 2008, **377**, 182-188.
- 35 J. A. Ho and R. D. Wauchope, *Anal. Chem.*, 2002, **74**, 1493-1496.
- 36 C.-W. Yen, H. de Puig, J. Tam, J. Gómez-Márquez, I. Bosch, K. Hamad-Schifferli and L. Gehrke, *Lab Chip*, 2015, **15**, 1638-1641.
- 37 M. Ornatska, E. Sharpe, D. Andreescu and S. Andreescu, *Anal. Chem.*, 2011, **83**, 4273-4280.
- 38 J. Hu, L. Wang, F. Li, Y. Han, M. Lin, T. Lu and F. Xu, *Lab Chip*, 2013, **13**, 4352-4357.
- 39 L. Rivas, A. de la Escosura-Muñiz, L. Serrano, L. Altet, O. Francino, A. Sánchez and A. Merkoçi, *Nano Res.*, 2015, **8**, 3704-3714.

- 40 D. H. Choi, S. K. Lee, Y. K. Oh, B. W. Bae, S. D. Lee, S. Kim, Y. B. Shin and M. G. Kim, *Biosens. Bioelectron.*, 2010, **25**, 1999-2002.
- 41 Z. Mei, W. Qu, Y. Deng, H. Chu, J. Cao, F. Xue, L. Zheng, H. S. El-Nezamic, Y. Wu and W. Chen, *Biosens. Bioelectron.*, 2013, **49**, 457-461.
- 42 C. Ge, L. Yu, Z. Fang and L. Zeng, *Anal. Chem.*, 2013, **85**, 9343-9349.
- 43 H. Xu, J. Chen, J. Birrenkott, J. Zhao, S. Takalkar, K. Baryeh and G. Liu, *Anal. Chem.*, 2014, **86**, 7351-7359.
- 44 G. Shen, H. Xu, A.S. Gurung, Y. Yang and G. Liu, *Anal. Sci.*, 2013, **29**, 799-804.
- 45 H. Ye, K. Yang, J. Tao, Y. Liu, Q. Zhang, S. Habibi, Z. Nie and X. Xia, *ACS Nano*, 2017, **11**, 2052-2059.
- 46 S. Gupta, S. Huda, P. K. Kilpatrick and O. D. Velev, *Anal. Chem.*, 2007, **79**, 3810-3820.
- 47 R. Hermann, P. Walther and M. Müller, *Histochem. Cell Biol.*, 1996, **106**, 31-39.
- 48 C. Oliver, *Methods Mol. Biol.*, 2010, **588**, 311-316.
- 49 T. A. Taton, C. A. Mirkin and R. L. Letsinger, *Science*, 2000, **289**, 1757-1760.
- 50 X. Liu, M. Atwater, J. Wang and Q. Huo, *Colloids Surf. B*, 2007, **58**, 3-7.
- 51 W. Yang, X. Li, G. Liu, B. Zhang, Y. Zhang, T. Kong, J. Tang, D. Li and Z. Wang, *Biosens. Bioelectron.*, 2011, **26**, 3710-3713.
- 52 L. Anfossi, F. Di Nardo, C. Giovannoli, C. Passini and C. Baggiani, *Anal. Bioanal. Chem.*, 2013, **405**, 9859-9867.
- 53 M. O. Rodríguez, L. B. Covián, A. C. García and M. C. Blanco-López, *Talanta*, 2016, **148**, 272-278.
- 54 Z. Ma and S.-F. Sui, *Angew. Chem. Int. Ed.*, 2002, **41**, 2176-2179.
- 55 E. Fu, T. Liang, J. Houghtaling, S. Ramachandran, S. A. Ramsey, B. Lutz and P. Yager, *Anal. Chem.*, 2011, **83**, 7941-7946.
- 56 Y. Xia, Y. Xiong, B. Lim and S. E. Skrabalak, *Angew. Chem. Int. Ed.*, 2009, **48**, 60-103.
- 57 M. Kumar, R. Kumar and V. Bhalla, *Org. Lett.*, 2010, **13**, 366-369.
- 58 P. Miao, L. Ning, and X. Li, *Anal. Chem.*, 2013, **85**, 7966-7970.
- 59 J. Park, S. Choi, T. I. Kim and Y. Kim, *Analyst*, 2012, **137**, 4411-4414.
- 60 A. Habib and M. Tabata, *J. Inorg. Biochem.*, 2004, **98**, 1696-1702.
- 61 R. A. Sheldon and S. Van Pelt, *Chem. Soc. Rev.*, 2013, **42**, 6223-6235.
- 62 L. Gao, J. Zhuang, L. Nie, J. Zhang, Y. Zhang, N. Gu, T. Wang, J. Feng, D. Yang, S. Perrett

- and X. Yan, *Nat. Nanotechnol.*, 2007, **2**, 577.
- 63 C. P. Price and D. J. Newman, Eds. *Principles and Practice of Immunoassay, 2nd ed.*, Stockton, New York, 1997.
- 64 R. M. Lequin, *Clin. Chem.*, 2005, **51**, 2415-2418.
- 65 D. Wild, *The Immunoassay Handbook, 4th ed.*, Elsevier, Amsterdam, 2013.
- 66 X. Mao, Y. Ma, A. Zhang, L. Zhang, L. Zeng and G. Liu, *Anal. Chem.*, 2009, **81**, 1660-1668.
- 67 Y. He, S. Zhang, X. Zhang, M. Baloda, A. S. Gurung, H. Xu, X. Zhang and G. Liu, *Biosens. Bioelectron.*, 2011, **26**, 2018-2024.
- 68 C. Parolo, A. de la Escosura-Muñiz and A. Merkoçi, *Biosens. Bioelectron.*, 2013, **40**, 412-416.
- 69 H. Wei and E. Wang, *Chem. Soc. Rev.*, 2013, **42**, 6060-6093.
- 70 E. Kuah, S. Toh, J. Yee, Q. Ma and Z. Gao, *Chem. Eur. J.*, 2016, **22**, 8404-8430.
- 71 Z. Gao, M. Xu, L. Hou, G. Chen and D. Tang, *Anal. Chim. Acta*, 2013, **776**, 79-86.
- 72 X. Xia, J. Zhang, N. Lu, M. J. Kim, K. Ghale, Y. Xu, E. McKenzie, J. Liu and H. Ye, *ACS Nano*, 2015, **9**, 9994-10004.
- 73 H. Ye, Y. Liu, A. Chhabra, E. Lilla and X. Xia, *ChemNanoMat*, 2017, **3**, 33-38.
- 74 W. He, X. Wu, J. Liu, X. Hu, K. Zhang, S. Hou, W. Zhou and S. Xie, *Chem. Mater.*, 2010, **22**, 2994.
- 75 M. Ma, Y. Zhang and N. Gu, *Colloids Surf. A*, 2011, **373**, 6-10.
- 76 P. V. Iyer and L. Ananthanarayan, *Process Biochem.*, 2008, **43**, 1019-1032.
- 77 Z. Gao, H. Ye, D. Tang, J. Tao, S. Habibi, A. Minerick, D. Tang and X. Xia, *Nano Lett.*, 2017, **17**, 5572-5579.
- 78 C. N. Loynachan, M. R. Thomas, E. R. Gray, D. A. Richards, J. Kim, B. S. Miller, J. C. Brookes, S. Agarwal, V. Chudasama, R. A. McKendry and M. M. Stevens, *ACS Nano*, 2018, **12**, 279-288.
- 79 T. Jiang, Y. Song, D. Du, X. Liu and Y. Lin, *ACS Sens.*, 2016, **1**, 717-724.
- 80 J. Chen, S. Zhou and J. Wen, *Anal. Chem.*, 2014, **86**, 3108-3114.
- 81 C. Liu, Q. Jia, C. Yang, R. Qiao, L. Jing, L. Wang, C. Xu and M. Gao, *Anal. Chem.*, 2011, **83**, 6778-6784.
- 82 Y. Xia, X. Xia and H. C. Peng, *J. Am. Chem. Soc.*, 2015, **137**, 7947-7966.
- 83 Y. Xia, K. D. Gilroy, H. C. Peng and X. Xia, *Angew. Chem. Int. Ed.*, 2017, **56**, 60-95.

- 84 P. D. Howes, R. Chandrawati and M. M. Stevens, *Science*, 2014, **346**, 1247390.
- 85 J. Shu, Z. Qiu, S. Lv, K. Zhang and D. Tang, *Anal. Chem.*, 2018, **90**, 2425-2429.
- 86 Z. Qiu, J. Shu and D. Tang, *Anal. Chem.*, 2017, **90**, 1021-1028.
- 87 X. Huang, Y. Liu, B. Yung, Y. Xiong and X. Chen, *ACS nano*, 2017, **11**, 5238-5292.
- 88 J. Shu and D. Tang, *Chem. -Asian J.*, 2017, **12**, 2780-2789.
- 89 D. Mark, S. Haeberle, G. Roth, F. Von Stetten and R. Zengerle, *Chem. Soc. Rev.*, 2010, **39**, 1153-1182.
- 90 C. D. Chin, T. Laksanasopin, Y. K. Cheung, D. Steinmiller, V. Linder, H. Parsa, J. Wang, H. Moore, R. Rouse, G. Umvilighozo and E. Karita, *Nat. Med.*, 2011, **17**, 1015.
- 91 A. W. Martinez, S. T. Phillips, G. M. Whitesides and E. Carrilho, *Anal. Chem.*, 2010, **82**, 3-10.
- 92 D. J. You, T. San Park and J. Y. Yoon, *Biosens. Bioelectron.*, 2013, **40**, 180-185.
- 93 D. H. Kim, R. Ghaffari, N. Lu and J. A. Rogers, *Annu. Rev. Biomed. Eng.*, 2012, **14**, 113-128.
- 94 D. D. Liana, B. Raguse, J. J. Gooding and E. Chow, *Sensors*, 2012, **12**, 11505-11526.
- 95 E. Pilavaki and A. Demosthenous, *Sensors*, 2017, **17**, 2673.
- 96 S. K. Vashist, P. B. Luppa, L. Y. Yeo, A. Ozcan and J. H. Luong, *Trends Biotechnol.*, 2015, **33**, 692-705.

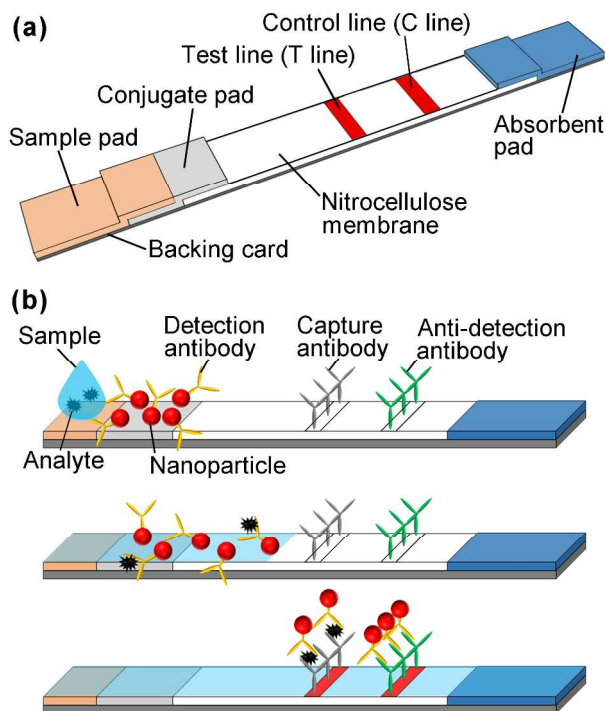


**Figure 1.** Schematics showing the general principle of a lateral flow assay (LFA). (a) Major components of a LFA test strip; and (b) Events involved in a sandwich-type LFA of analytes, in which analyte-bound nanoparticle labels are captured by antibodies in test line (signal of detection) and control line (proof of validity).

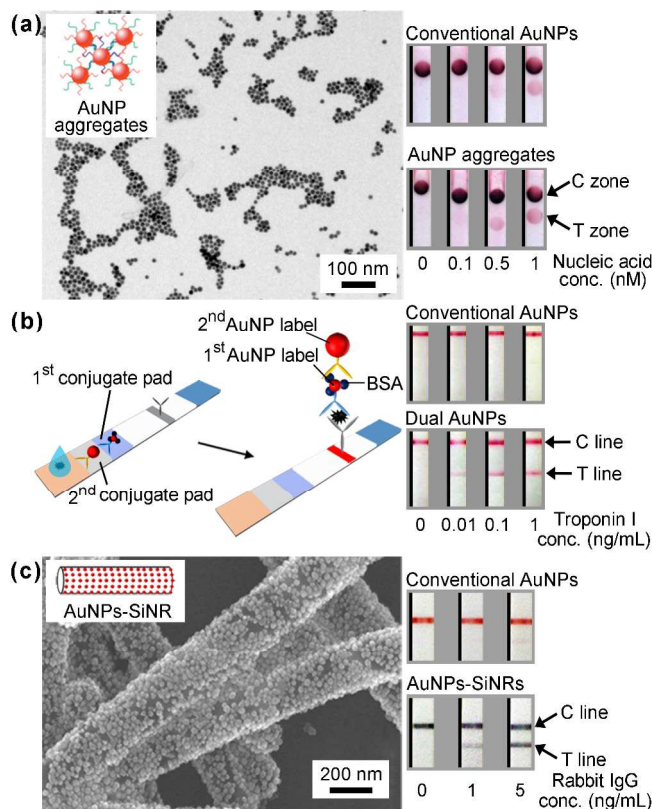


**Figure 2.** Amplifying the detection signal of Au nanoparticles (AuNPs)-based colorimetric lateral flow assay (CLFA) through the uses of: (a) AuNP aggregates as the labels; (b) two AuNP labels with different sizes; and (c) AuNPs decorated silica nanorods (SiNRs) as the labels. Performance of these three CLFAs in detecting model analytes are compared with conventional AuNPs-based CLFAs (see the right columns). (a-c) were adapted and reproduced from Refs. 38, 40, and 43, respectively, with permissions from the Royal Society of Chemistry, Elsevier, and Copyright 2014 American Chemical Society (ACS).

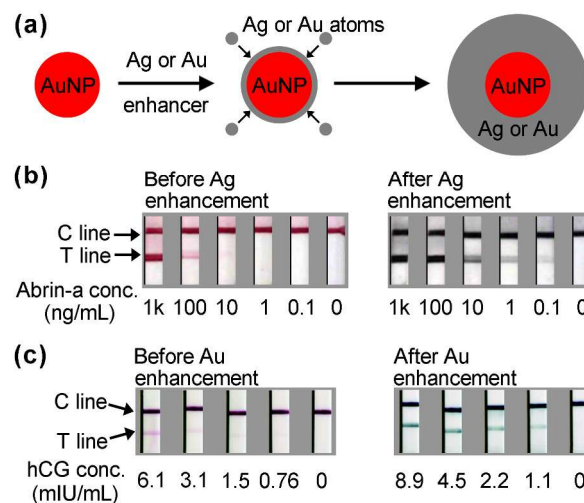


**Figure 3.** Silver and gold enhancement techniques for enhancing the signal of AuNPs-based CLFA. (a) Schematics showing the mechanisms of silver and gold enhancements. AuNPs act as catalysts to accelerate the reaction in an enhancer solution (*i.e.*, reduction of Ag or Au precursor by a reducing agent). The newly formed Ag or Au atoms are deposited on the surface of initial AuNPs, during which particle size is enlarged; (b, c) Representative examples showing the performance of silver and gold enhancements-coupled CLFAs, respectively, in detecting model analytes. (b) and (c) were adapted and reproduced from Refs. 51 and 55, respectively, with permissions from the Elsevier and Copyright 2011 American Chemical Society (ACS).



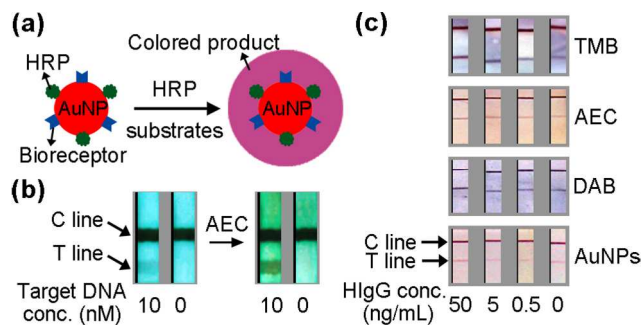


**Figure 4.** Signal amplification for CLFA by using HRPs- and bioreceptors-dually functionalized AuNPs as the labels. (a) Schematics showing the mechanism of signal amplification, where HRPs effectively generate colored products by catalyzing chromogenic substrates; (b) Detection results of a target DNA by the HRP-assisted CLFA. 3-amino-9-ethyl-carbazole (AEC) was chosen as a HRP substrate; (c) a comparison study of different HRP substrates (including TMB, AEC, and DAB) in HRP-assisted CLFA, where AuNPs-based CLFA was set as a benchmark. (b) and (c) were adapted and reproduced from Refs. 66 and 68, respectively, with permissions from the Copyright 2009 American Chemical Society (ACS) and Elsevier.

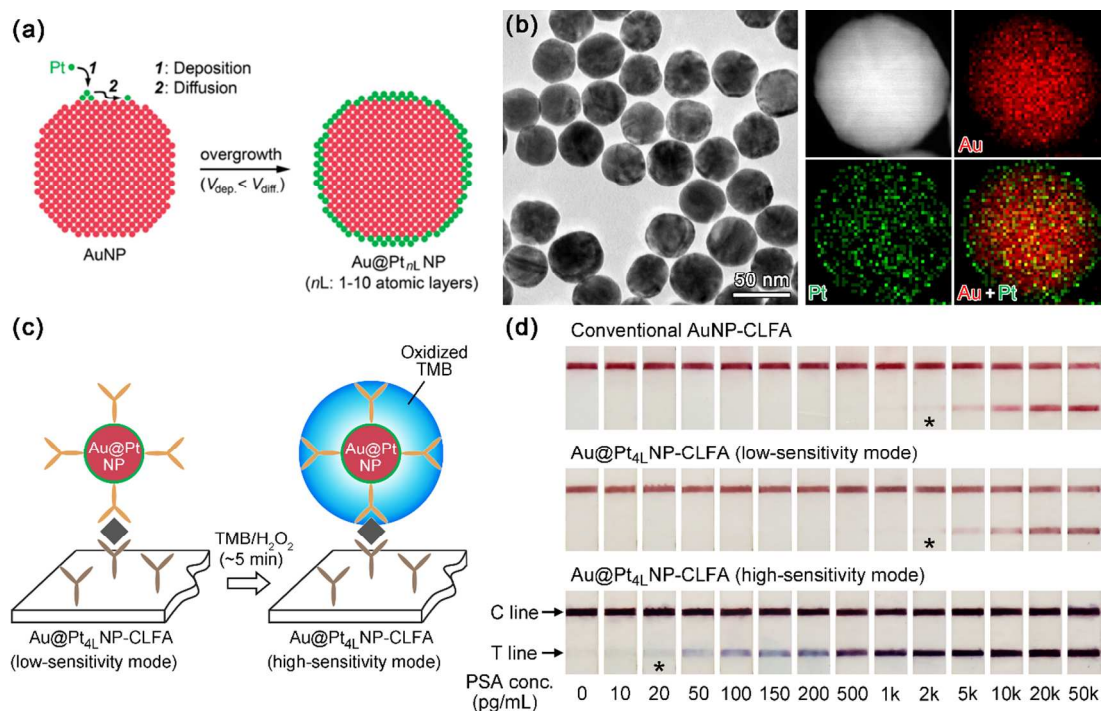


**Figure 5.** Au@Pt<sub>nL</sub> core@shell NPs (*nL*: 1-10 atomic layers) as a type of novel label for CLFA. (a) Schematics showing the fabrication of Au@Pt<sub>nL</sub> NPs. Pt atoms resulted from the reduction of a Pt precursor are deposited onto an AuNP to form a conformal Pt shell with thicknesses of 1-10 atomic layers; (b) Representative transition electron microscope image (left) and energy-dispersive X-ray (EDX) mapping image (right) of Au@Pt<sub>4L</sub> NPs as a representative sample; (c) Schematics showing the utilization of Au@Pt<sub>4L</sub> NPs as labels in CLFA for signal amplification. In the "low-sensitivity mode", the color signal (red) arises from the plasmonic AuNP cores. In the "high-sensitivity mode", a secondary color signal (blue) is generated from Pt shells as highly efficient peroxidase mimics; (d) Detection results of prostate-specific antigen (PSA) standards by conventional AuNP-CLFA and the Au@Pt<sub>4L</sub> NP-CLFA under two different modes. The asterisks (\*) indicate detection limits by the naked eye. Adapted and reproduced from Ref. 77 with permission from the Copyright 2017 American Chemical Society (ACS).